CEP120-mediated KIAA0753 recruitment onto centrioles is required for timely neuronal differentiation and germinal zone exit in the developing cerebellum

Chia-Hsiang Chang, Ting-Yu Chen, I-Ling Lu, Rong-Bin Li, Jhih-Jie Tsai, Pin-Yeh Lin, and Tang K. Tang

Institute of Biomedical Sciences, Academia Sinica, Taipei 11529, Taiwan

Joubert syndrome (JS) is a recessive ciliopathy in which all affected individuals have congenital cerebellar vermis hypoplasia. Here, we report that CEP120, a JS-associated protein involved in centriole biogenesis and cilia assembly, regulates timely neuronal differentiation and the departure of granule neuron progenitors (GNPs) from their germinal zone during cerebellar development. Our results show that depletion of Cep120 perturbs GNP cell cycle progression, resulting in a delay of cell cycle exit in vivo. To dissect the potential mechanism, we investigated the association between CEP120 interactome and the JS database and identified KIAA0753 (a JS-associated protein) as a CEP120-interacting protein. Surprisingly, we found that CEP120 recruits KIAA0753 to centrioles, and that loss of this interaction induces accumulation of GNPs in the germinal zone and impairs neuronal differentiation. Importantly, the replenishment of wild-type CEP120 rescues the above defects, whereas expression of JS-associated CEP120 mutants, which hinder KIAA0753 recruitment, does not. Together, our data reveal a close interplay between CEP120 and KIAA0753 for the germinal zone exit and timely neuronal differentiation of GNPs during cerebellar development, and mutations in *CEP120* and *KIAA0753* may participate in the heterotopia and cerebellar hypoplasia observed in JS patients.

[*Keywords*: Cep120; cerebellar development; Joubert syndrome; Kiaa0753; centrioles; granule neuron progenitors; moonraker; neuronal differentiation]

Supplemental material is available for this article.

Received May 5, 2021; revised version accepted September 28, 2021.

The cerebellum develops vigorously during postnatal stages. The peak period for granule neuron progenitor (GNP) proliferation is around postnatal days 5–8; this leads to the genesis of billions of granule neurons, the most abundant type of cell in the central nervous system (CNS) (Hatten and Roussel 2011). GNPs proliferate exuberantly in the external granular layer (EGL) when they meet with the mitogen, Sonic Hedgehog (SHH), which is secreted by Purkinje cells (Dahmane and Ruiz-i-Altaba 1999; Wallace 1999; Wechsler-Reya and Scott 1999). After several rounds of symmetric cell division, GNPs exit their germinal zone and migrate through the molecular layer (ML) along the radial fibers of Bergmann glial cells (Edmondson and Hatten 1987) to the internal granular layer (IGL), where they terminally differentiate into mature granule neurons.

The primary cilium has been in the spotlight recently: It is required for vertebrate cells to sense SHH signaling and thereby governs the expansion of GNPs (Chizhikov et al. 2007). Ablation of primary cilia by conditional knockout of Kif3a, a kinesin-II motor protein required for ciliogenesis, leads to underdevelopment of the cerebellum and significantly reduces the number of proliferating GNPs (Spassky et al. 2008). Consistently, abnormalities in primary cilia result in several developmental disorders of the cerebellum, such as Joubert syndrome (JS), a rare autosomal recessive genetic disorder that affects the cerebellum and brain stem (Braun and Hildebrandt 2017).

Our group and others previously showed that CEP120 is a daughter centriole-enriched protein (Mahjoub et al. 2010) that participates in the process of centriole elongation (Comartin et al. 2013; Lin et al. 2013). We further demonstrated that CEP120 interacts not only with CPAP for centriole elongation (Lin et al. 2013), but also with C2CD3 and Talpid3 for centriole appendage assembly and ciliogenesis (Tsai et al. 2019). Interestingly,

Corresponding author: tktang@ibms.sinica.edu.tw
Article published online ahead of print. Article and publication date are online at http://www.genesdev.org/cgi/doi/10.1101/gad.348636.121.

CPAP mutations are reported to cause autosomal recessive primary microcephaly (Woods et al. 2005), while *CEP120* mutations have been identified in complex ciliopathy phenotypes in humans, including JS, Meckel-Gruber syndrome, and short-rib thoracic dysplasia (Shaheen et al. 2015; Roosing et al. 2016). Remarkably, in vivo studies in murine models showed that conditional knockout of *Cpap* or *Cep120* in the cerebellum impairs ciliogenesis in neurons, leading to severe cerebellar hypoplasia (Wu et al. 2014; Lin et al. 2020). Although these genes have been relatively well studied in the cerebral cortex by tracing the behaviors of individual neural progenitors in vivo (Xie et al. 2007; Garcez et al. 2015), the literature lacks detailed investigations of these genes in the developing cerebellum. Given that *CEP120* mutations are detrimental for cerebellar morphogenesis in JS (Roosing et al. 2016) and CEP120 is highly expressed in actively proliferating GNPs of the human fetal cerebellum (Powell et al. 2020), a thorough examination of the cell-autonomous effects of CEP120 in cerebellar GNPs is crucial for understanding the neuropathology of JS.

In the current study, we used in vivo cerebellar electroporation to monitor the neurogenesis of cerebellar GNPs with spatiotemporal precision. We observed that Cep120 depletion delays the germinal zone exit of GNPs. Mechanistically, we found that the proper CEP120-mediated recruitment of another JS protein, KIAA0753, to the centriole is important for the correct timing of GNP differentiation and germinal zone exit. Our findings reveal a novel cellular and molecular mechanism implemented by two JS proteins, Cep120 and Kiaa0753, for the pathogenesis of JS.

Results

Cep120 *knockdown delays the departure of GNPs from their germinal zone in vivo*

To study the role of Cep120 in cerebellar GNPs, we packaged into lentiviruses a control short hairpin RNA (sh-RNA) along with a green fluorescent protein (GFP) reporter (termed sh-Ctrl-GFP) or four different sh-RNAs targeting mouse *Cep120* (sh-*Cep120*-GFP #1–4). GNPs were isolated from the postnatal day 6 (P6) murine cerebellum and infected with lentiviruses carrying the various sh-RNAs. Of them, sh-*Cep120* #1 and #3 repeatedly yielded significant reduction of the Cep120 protein level (Supplemental Fig. S1A,B). Regarding the efficacy of these two sh-RNAs, we first tested whether the percentage of ciliated GNPs was affected upon Cep120 knockdown (KD) at 3 d after infection when the Cep120 protein level was notably reduced (Supplemental Fig. S1C,D). We observed that a quarter of the proliferative GNPs (identified by positivity for cyclin D1$^+$ [Ccnd1]) in the sh-Ctrl group possessed a primary cilium (marked by Arl13b), whereas this population was largely decreased in GNPs infected with two sh-RNAs targeting *Cep120*, and their cilium length was also reduced (Supplemental Fig. S1E–G). Thus, *Cep120* KD effectively reduced ciliated GNPs in vitro. We further validated that *Cep120* KD, triggered through cerebellar electroporation in vivo, diminished the presence of Cep120$^+$ signals on centrosomes (Supplemental Fig. S1H–J), and decreased the percentage of ciliated GNPs and their ciliary length at days 1 and 2 in the EGL (Supplemental Fig. S1K–P). We thus selected these two sh-RNAs (sh-*Cep120* #1 and #3) for our subsequent studies.

To investigate the function of Cep120 in cerebellar GNPs in a cell-autonomous manner, we performed in vivo cerebellar electroporation at P6 using sh-Ctrl, sh-*Cep120* #1, or sh-*Cep120* #3 along with a GFP vector (pCMV-enhanced β-actin promoter-IRES-GFP; termed pCIG2), and then traced the labeled neurons at days 1 (D1), 2 (D2), and 4 (D4) thereafter. Both the control and *Cep120* KD neurons were observed in the EGL at D1 (Supplemental Fig. S2A,B, P6 D1), indicating that these neurons began at the same starting point. At D2, ~20% of GFP$^+$ neurons in all groups had migrated to the IGL and extended their parallel fibers between the EGL and ML (Supplemental Fig. S2A,B, P6 D2). Surprisingly, *Cep120* KD at D4 (Supplemental Fig. S2C) led to an accumulation of GFP$^+$ GNPs in the EGL, when most of the control cells (sh-Ctrl) had reached the IGL, their destination during cerebellar development (Fig. 1A). Importantly, this KD effect was effectively rescued by supplying with a sh-RNA-resistant human *CEP120* (pCIG2-*hCEP120*), suggesting that this phenotype is specific to the reduction of *Cep120* expression (Fig. 1A).

To determine the molecular signatures in these ectopic-accumulating neurons seen under *Cep120* KD, we coimmunostained cerebellar sections for a differentiated neuronal marker (Tuj1) and a mature neuronal marker (NeuN) at D4. At this time point, Tuj1$^-$NeuN$^-$ cells were rarely seen in control cerebella but were significantly increased in *Cep120* KD cerebella (Fig. 1B; Supplemental Fig. S2D). This suggests that the loss of Cep120 is associated with the retention of more undifferentiated cells (Tuj1$^-$NeuN$^-$) in the EGL. The presence of Ki67 (a cell proliferation marker) in the EGL has been reported to be a reliable indicator for GNPs in vivo (Nakashima et al. 2015). Here, we found that *Cep120* KD cerebella exhibited more Ki67$^+$Tuj1$^-$ cells in the EGL than control cerebella (Fig. 1C; Supplemental Fig. S2E) at D4, suggesting that these undifferentiated cells (Ki67$^+$Tuj1$^-$NeuN$^-$) are still GNPs. Together, our results indicate that Cep120 is required for the ability of GNPs to leave their germinal zone in the developing cerebellum.

Cep120 regulates GNP differentiation and cell cycle exit in vivo

We next investigated whether the accumulation of GNPs in the EGL resulted from the differentiation delay seen under *Cep120* KD. To test this hypothesis, we collected P6 cerebella at D2 after electroporation, a critical time point at which GNPs are largely undergoing differentiation in vivo (Nakashima et al. 2015). In line with our observation at D4, we detected more Ki67$^+$ cells (representing GNPs) in cells expressing *Cep120* sh-RNAs-GFP compared with sh-Ctrl-GFP (Supplemental Fig. S3) at D2. Importantly, coelectroporation of *Cep120* sh-RNAs with pCIG2 vector

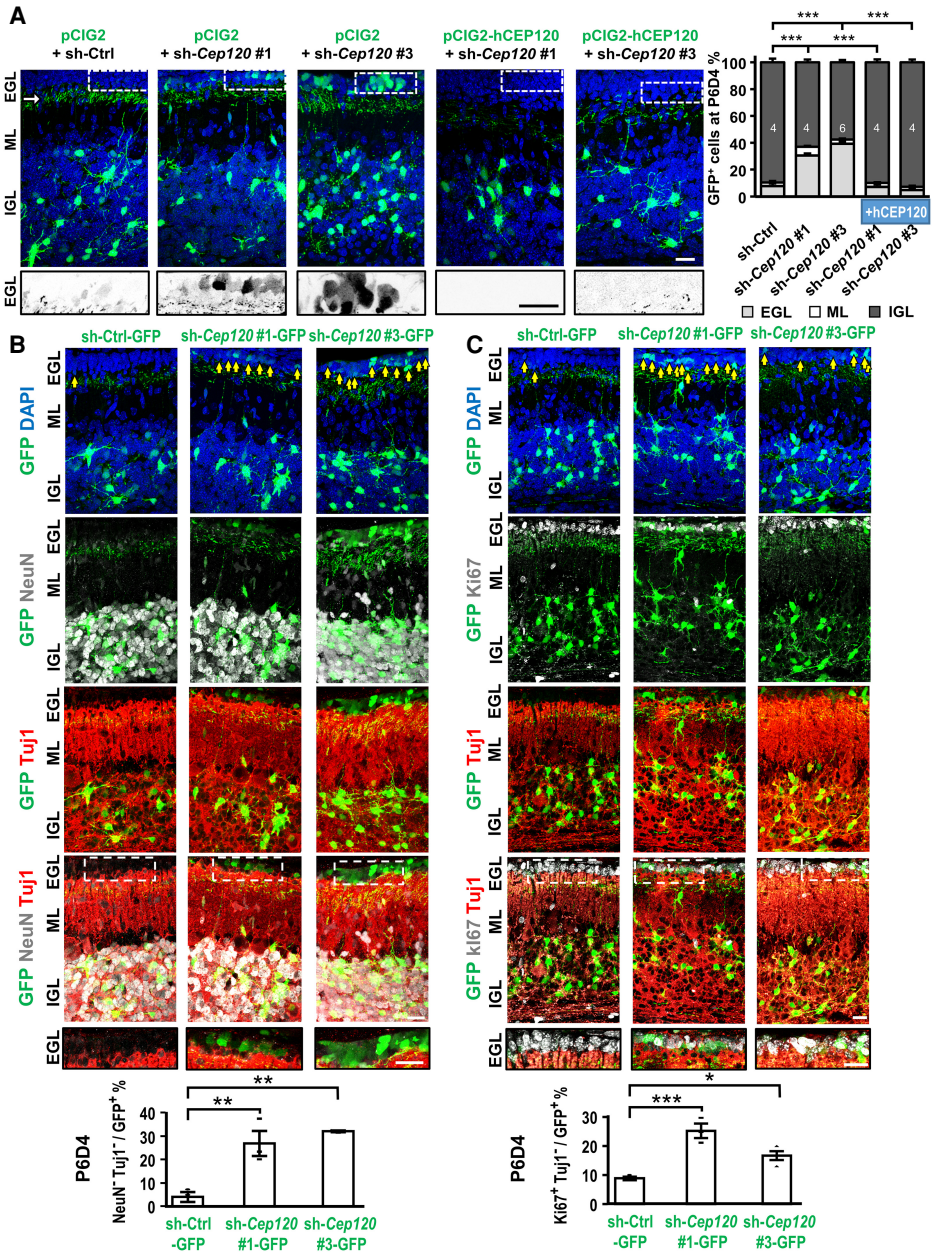

Figure 1. *Cep120* KD delays the departure of GNPs from their germinal zone in vivo. (*A*) P6 cerebella were electroporated with the indicated plasmids, collected at D4, and counterstained with DAPI (blue). An arrow indicates parallel fibers extending from granule neurons. GFP signals in boxed regions are enlarged at the *bottom* (black–white). Scale bar, 20 µm. (EGL/IGL) External/Internal granular layer, (ML) molecular layer. The bar graph displays the distribution of GFP$^+$ cells at P6 D4. Numbers in the bar represent the animals used for each group, and >500 neurons were counted per group. (*B*,*C*) Differentiation status of *Cep120* knockdown GNPs at P6 D4. P6 cerebella were electroporated with the indicated plasmids, collected at D4, and immunostained for NeuN (a mature neuron marker; white in *B*) or Ki67 (a progenitor cell marker; white in *C*), along with Tuj1 (a differentiated neuronal marker; red), and DAPI (blue). Boxed regions are enlarged at the *bottom*. Yellow arrows indicate NeuN$^-$Tuj1$^-$ (*B*) and Ki67$^+$Tuj1$^-$ (*C*) cells. Scale bar, 20 µm. The bar graph displays the percentage of immature neurons (NeuN$^-$Tuj1$^-$; *B*), and progenitor cells (Ki67$^+$Tuj1$^-$; *C*) among GFP$^+$ cells at D4. At least three animals and >500 neurons were counted per group.

displayed a similar phenotype, while this phenotype was restored by coelectroporating human *CEP120* (pCIG2-*hCEP120*), indicating that the increased GNP population in the EGL was specific to *Cep120* KD (Fig. 2A). In addition, loss of *Cep120* decreased the percentage of Neurod1$^+$ cells (a neuronal differentiation marker) in the inner EGL (iEGL) at D2 compared with the level seen in control cerebella (Fig. 2B). Taken together, our results indicate that Cep120 depletion perturbs the transition of GNPs to differentiating neurons.

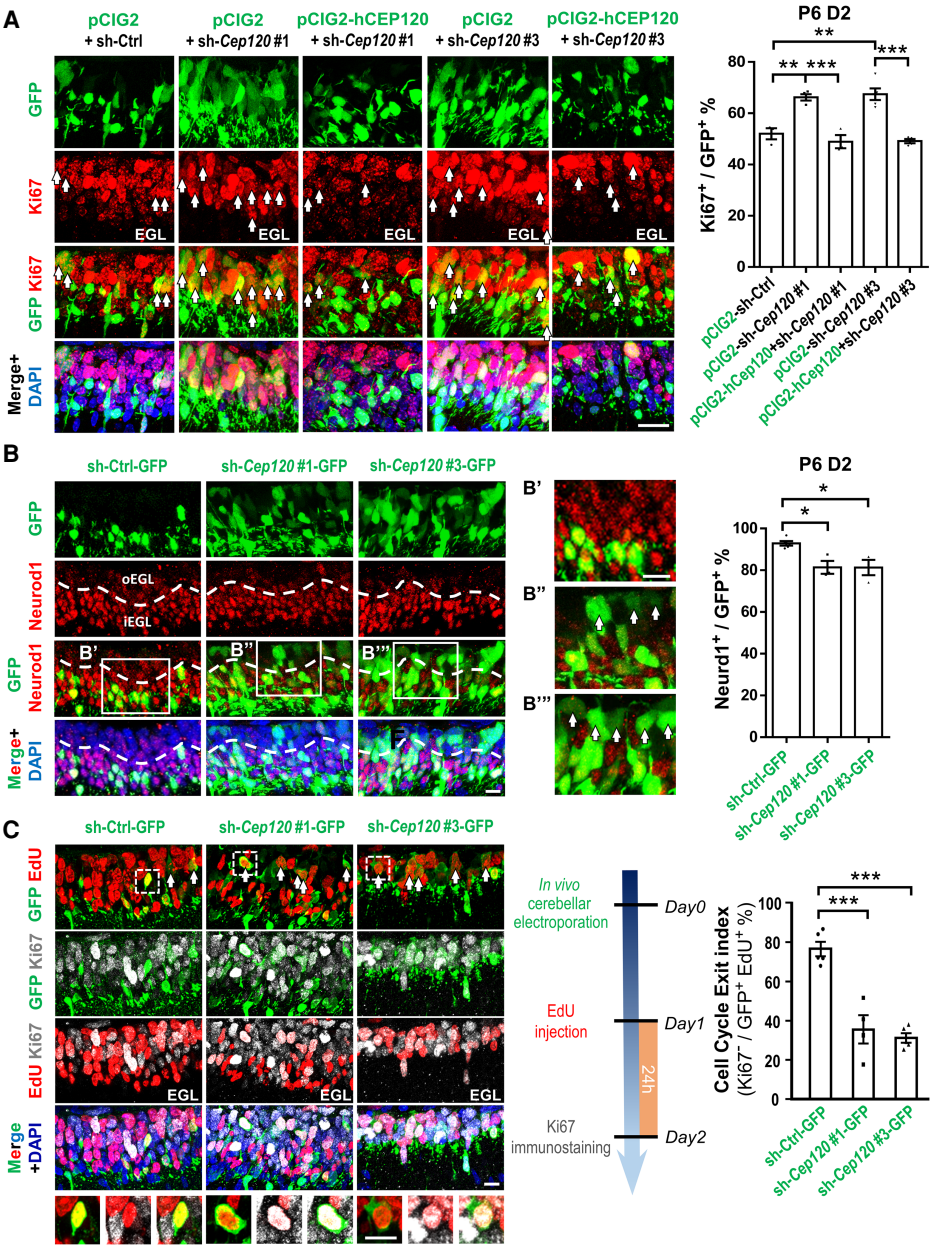

Figure 2. Cep120 is required for differentiation and cell cycle exit of GNPs in vivo. (*A*) P6 cerebella were electroporated with the indicated plasmids, collected at D2, and immunostained for Ki67 (red) and DAPI (blue). (Arrows) Ki67$^+$GFP$^+$ cells in the EGL. Scale bar, 20 µm. At least three animals and >500 neurons were included per group. (*B*) P6 cerebella were electroporated with the indicated plasmids, collected at D2, and immunostained for Neurod1 (red) and DAPI (blue). Dashed lines mark the boundary between the outer EGL (oEGL) and inner EGL (iEGL). Boxed regions are enlarged at *right*. (Arrows) Neurod1$^-$ GFP$^+$ cells. Scale bar, 10 µm. At least three animals and >300 neurons were counted per group. (*C*) Assay for cell cycle exit. (*Left* panel) P6 cerebella were electroporated with the indicated plasmids and treated as shown in the *middle* panel. Cerebellar sections were immunostained with EdU (red), Ki67 (white), and DAPI (blue). Scale bar, 10 µm. (Arrows) Ki67$^+$ GFP$^+$EdU$^+$ cells in the EGL. Boxed regions with separated channels are enlarged at the *bottom*. (*Middle* panel) Scheme for the cell cycle exit assay. (*Right* panel) The bar graph represents the index of cell cycle exit. At least three animals and >400 neurons were examined per group.

Since GNPs exit the cell cycle prior to the onset of differentiation (Espinosa and Luo 2008; Nakashima et al. 2015), we performed 5-ethynyl-2′-deoxyuridine (EdU) injection at D1 after electroporation in vivo and monitored the cell cycle exit of the labeled proliferative GNPs. As the estimated cell cycle duration in GNPs is ~19 h in the postnatal murine cerebellum (Fujita 1967), we measured the cell cycle exit index at D2 (Sanada and Tsai 2005) and examined the percentage of Ki67$^-$ neurons among the GFP$^+$EdU$^+$ cells. As expected, most of GFP$^+$

EdU^+ control cells did not express Ki67 at D2; in contrast, *Cep120* KD cerebella exhibited numerous GFP^+ EdU^+ cells expressing Ki67 (Fig. 2C). This indicates that the cell cycle exit is impaired in *Cep120* KD GNPs in vivo.

Cep120 depletion perturbs the G1–S phase transition of GNPs in vivo and in vitro

To identify the potential cause for the blockade of cell cycle exit in *Cep120* KD GNPs, we performed organotypic slice culture at D2 after electroporation ex vivo, and traced individual GNPs during their neurogenesis. Within a 6-h observation period, the progeny cells of sh-Ctrl-GFP-treated GNPs frequently underwent a successful cell division and migrated away from the EGL. This event was largely abolished in *Cep120* KD GNPs (sh-*Cep120*-GFP #1) (Fig. 3A,B; Supplemental Movies S1, S2), suggesting that the reduction of mitotic events was coupled to the defective germinal zone exit (Fig. 1A) when the Cep120 protein level is reduced at this timing (Fig. 3C). Indeed, by examining the mitotic index through phospho-histone H3 (pH3) staining at D2 in vivo, our results confirmed that the percentage of mitotic cells was substantially reduced in *Cep120* KD GNPs (Fig. 3D,E).

We speculated that the decreased mitotic index seen at D2 could have been derived from the cell cycle blockade at D1. To test this, we first immunostained the electroporated cells with Ki67 (a pan-cell cycle marker that labels GNPs at the EGL). We did not observe any significant difference in the $Ki67^+$ cells of the control and *Cep120* KD groups, indicating that the cells of these groups were in their proliferative cycle at D1 (Supplemental Fig. S4A,B). Under this condition, we labeled the S-phase cells and a portion of the G2/M-phase cells by injecting EdU for 3 h (Fig. 3F,G; Supplemental Fig. S4C) as previously described (Florio et al. 2012). The G2/M-phase cells were visualized by pH3 staining (Hendzel et al. 1997). Interestingly, drastically fewer electroporated S-phase cells were seen in the *Cep120* KD group compared with the control group at D1 (Fig. 3H), whereas there was no significant difference in the percentage of pH3-labeled G2/M-phase cells at this timing (Fig. 3I). Remarkably, the proportion of G0/G1-phase cells (EdU^-pH3^-/GFP^+) was largely increased upon *Cep120* KD (Fig. 3J). Taken together, these results show that the G1–S phase transition was impaired in *Cep120* KD GNPs at D1 in vivo, resulting in a subsequent reduction of mitotic events at D2, during cerebellar development.

To confirm these results in vitro, we infected purified GNPs with lentiviruses encoding sh-Ctrl-GFP or sh-*Cep120*-GFP for 3 d, followed by a pulse of EdU injection for 4 h. Repeatedly, we observed a decrease of EdU-incorporated cells among the cycling GNPs (GFP^+Ki67^+) in the *Cep120* KD group, suggesting that *Cep120* KD reduced cells entering into S and early G2/M phase in vitro (Supplemental Fig. S4D,E). Interestingly, Cep120 KD increased the EdU^- $pH3^-$ population (G0 and G1) among the GFP^+ cells, while the percentage of $Ki67^+$ cycling cells was similar between the control and *Cep120* KD groups at this stage (Supplemental Fig. S4F,G), suggesting that the increase of EdU^- $pH3^-$ cells upon *Cep120* KD was due to retaining more cells in the G1 phase. Thereafter, we detected a decreased mitotic index in *Cep120* KD GNPs in vitro (Supplemental Fig. S4H). Collectively, these results indicate that loss of Cep120 also delayed the G1–S phase transition in GNPs in vitro.

KIAA0753 is a CEP120-interacting protein involved in the departure of GNPs from their germinal zone in vivo

Since *CEP120* mutations are implicated in the pathogenesis of JS, we next aimed to identify potential disease-related CEP120-associated proteins by comparing two published CEP120 interactomes (Comartin et al. 2013; Gupta et al. 2015) with the known proteins involved in JS (MIM: PS213300). Among 45 potential CEP120-interacting proteins, TALPID3, C2CD3, OFD1, CSPP1, and KIAA0753 appeared on the list of JS-associated candidates (Fig. 4A). Our group and others had previously excluded OFD1 as a CEP120-interacting protein, and confirmed that C2CD3 (Tsai et al. 2019) and TALPID3 (Wu et al. 2014; Tsai et al. 2019) interact with CEP120. Here, our immunostaining results further show that Cep120 colocalized with C2cd3, Talpid3, Cspp1, and Kiaa0753 in the developing mouse cerebellum (Fig. 4B). To investigate the physical associations of these candidate proteins with CEP120, we performed coimmunoprecipitation (co-IP) experiments and found that CEP120-myc was able to form complexes with TALPID3-GFP and C2CD3-GFP, consistent with our previous report (Tsai et al. 2019); however, we were unable to detect CSPP1-GFP or its isoform, CSPPL-GFP (Patzke et al. 2006), in the co-IP complexes (Supplemental Fig. S5A). Importantly, we identified a novel physical association between CEP120 and KIAA0753 by reciprocal co-IP of their endogenous proteins in HEK293T cells and isolated GNPs (Fig. 4C; Supplemental Fig. S5B). Therefore, TALPID3, C2CD3, and KIAA0753 were selected for subsequent analysis.

To investigate whether these candidate proteins play crucial roles in the germinal zone exit of GNPs in vivo, we tested several sh-RNAs and small interfering RNAs (si-RNAs) targeting mouse *C2cd3*, *Talpid3*, and *Kiaa0753* for their efficiencies in reducing the targeted protein levels (Supplemental Fig. S5C–E). We also tested their abilities to reduce ciliogenesis in GNPs in vivo (Supplemental Fig. S5F–K), as the targeted genes have been implicated in ciliopathies (Hoover et al. 2008; Stephen et al. 2017; Wang et al. 2018; Fraser and Davey 2019). We then used the verified agents to perform KD of *C2cd3* (Fig. 4D) and *Talpid3* (Fig. 4E), and observed that GNPs exhibited distribution patterns similar to control GNPs at D4 after electroporation in vivo. Although the targeted proteins were effectively reduced at D4 in vivo (Supplemental Fig. S5L,M), C2cd3 and Talpid3 did not appear to affect the exit of GNPs from their germinal zone. Interestingly, loss of *Kiaa0753* in GNPs led to the accumulation of numerous GFP^+ cells in the EGL at D4 (Fig. 4E; Supplemental Fig. S5N), in a pattern similar to that seen with *Cep120* KD. Importantly, this phenotype was reversed by introducing an si-RNA-resistant human *KIAA0753* (pCIG2-h*KIAA0753*) (Fig. 4E), suggesting that

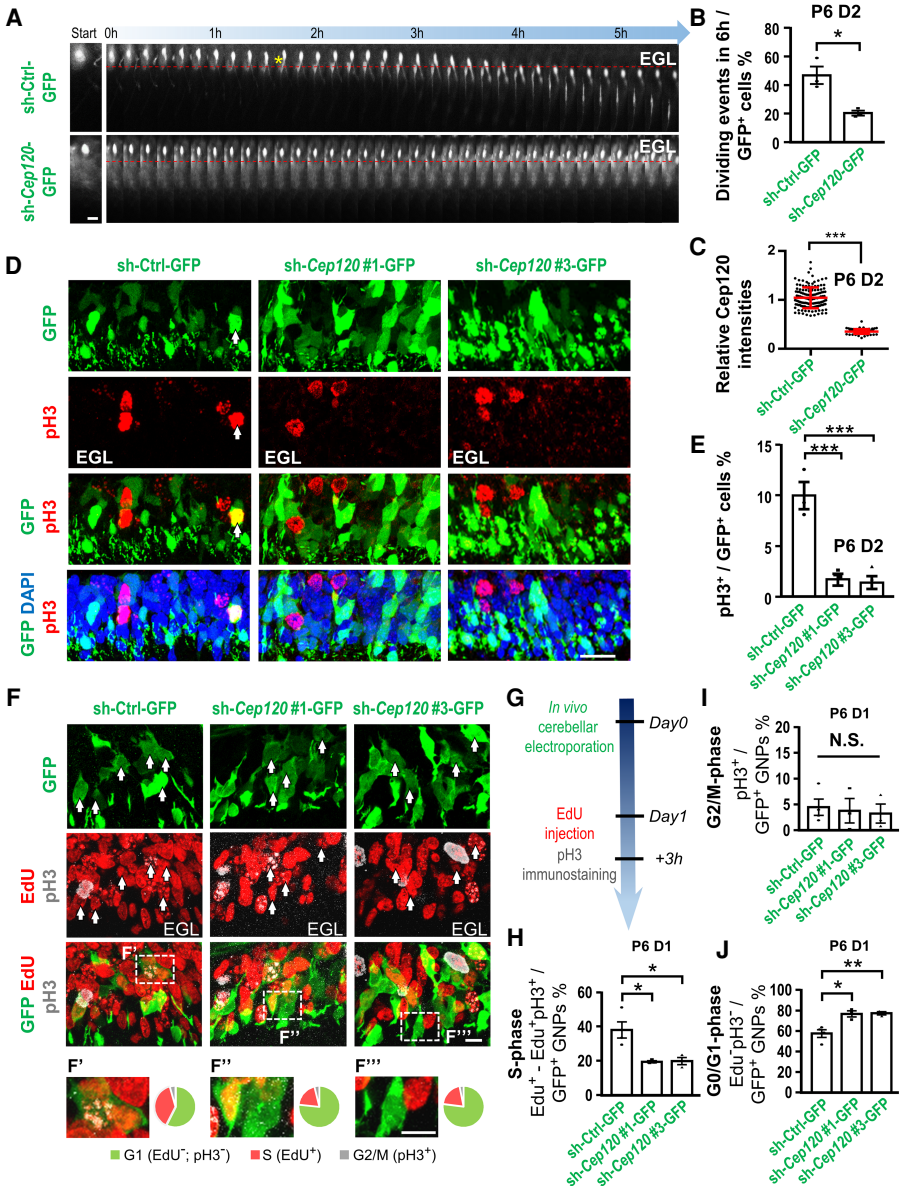

Figure 3. *Cep120* KD hinders cell cycle progression in GNPs in vivo. (*A*) The kymograph presents the behavior of GNP electroporated with the indicated plasmids from cerebellar organotypic slice culture at D2. (Yellow asterisk) A successful division of control GNP into two progeny cells, followed by neuronal migration away from the germinal zone. In contrast, sh-*Cep120*-treated GNPs did not divide appropriately for a prolonged period of time. Red dashed lines mark the boundary of the EGL. Scale bar, 10 µm. (*B*) The bar graph represents the percentage of mitotic events among GFP$^+$ cells within 6 h. Three animals and >50 neurons were traced per group. (*C*) The histogram displays the relative Cep120 intensities for each GFP$^+$ GNP at D2 after electroporation. More than 80 cells were measured in each group. (*D*) P6 cerebella were electroporated with the indicated plasmids, collected at D2, and immunostained for pH3 (red) and DAPI (blue). (Arrow) pH3$^+$ GFP$^+$ cells in EGL. Scale bar, 20 µm. (*E*) The bar graph represents the percentage of pH3$^+$ cells among the GFP$^+$ GNPs at P6 D2. Three animals and >500 neurons were investigated per group. (*F*) P6 cerebella were electroporated with the indicated plasmids and treated as shown in *G*. Cerebellar sections were immunostained with EdU (red), pH3 (white), and DAPI (blue). (Arrows) EdU$^+$ GFP$^+$ cells. Scale bar, 10 µm. Boxed regions are enlarged at the *bottom*. Pie charts represent the distribution of cell cycle phases. (*G*) Scheme for the cell cycle progression assay. (*H–J*) The bar graphs represent the percentage of S-phase cells (EdU$^+$ – EdU$^+$pH3$^+$; *H*), G2/M-phase cells (pH3$^+$; *I*), and G0/G1-phase cells (EdU$^-$pH3$^-$; *J*) among the GFP$^+$ cells. More than 400 neurons from three animals were examined per group.

this effect is specific to *KIAA0753* KD. Together, these findings indicate that Kiaa0753 is an important Cep120-interacting partner and that Kiaa0753, but not C2cd3 or Talpid3, plays a critical role in the exit of GNPs from their germinal zone in vivo.

Kiaa0753 *KD and* Cep120 *KD display similar phenotypes in the developing cerebellum*

Given that *Kiaa0753* KD delayed GNPs from leaving their germinal zone in the developing cerebellum, we next

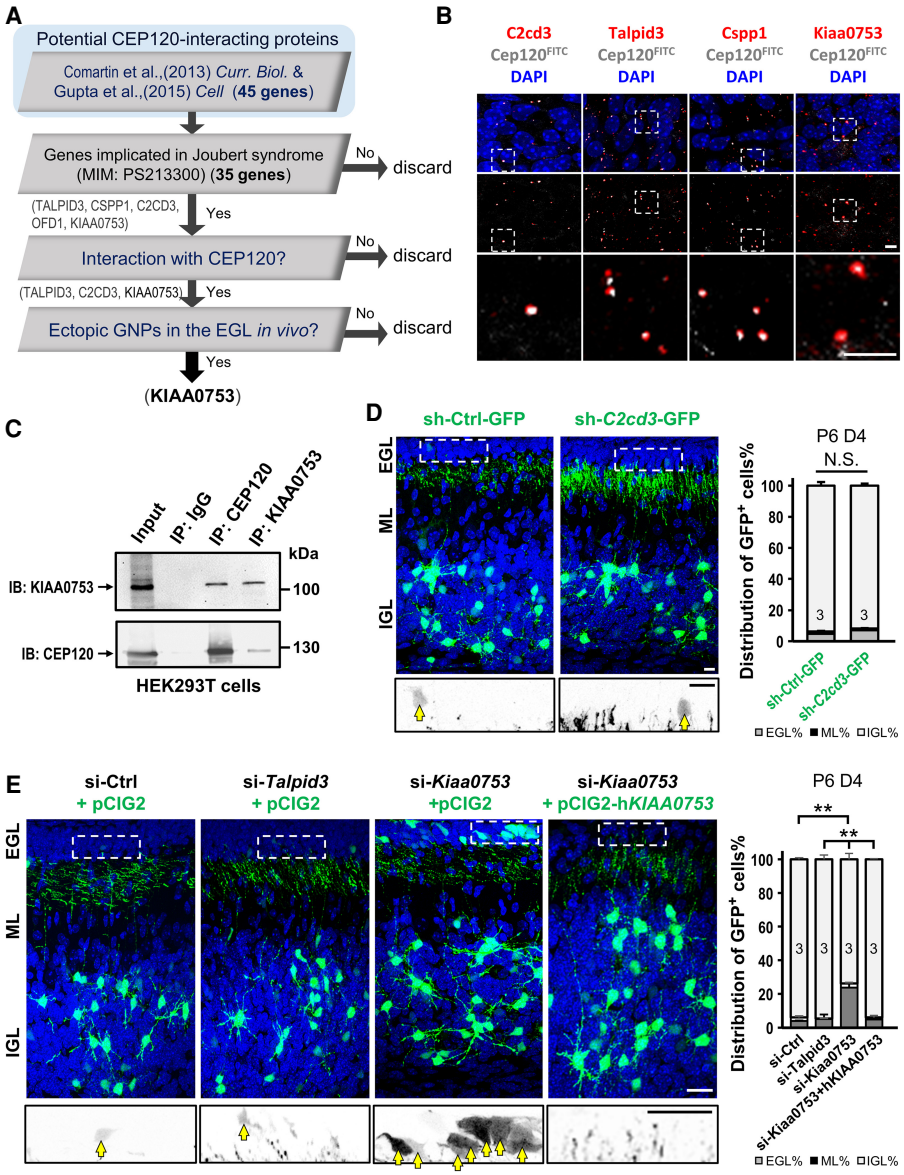

Figure 4. Kiaa0753 associates with Cep120 and regulates germinal zone exit in vivo. (*A*) A screening paradigm exhibiting the databases and exclusion criteria for searching potential Cep120-associated proteins that could regulate the germinal zone exit of GNPs. (*B*) P8 cerebellar sections were immunostained for C2cd3, Talpid3, Cspp1, or Kiaa0753 (red); FITC-tagged Cep120 (Cep120^{FITC}, white); and DAPI (blue). Scale bar, 5 µm. Boxed regions are enlarged at the *bottom*. (*C*) CEP120 physically associates with KIAA0753 in cells. Lysates from HEK293T cells were immunoprecipitated and then immunoblotted with the indicated antibodies. (*D*) P6 cerebella were electroporated with the indicated plasmids and collected at D4. GFP signals within the boxed regions are enlarged at the *bottom* (black). (Arrows) GFP$^+$ cell body in the EGL. The spike-like black signals surrounding arrows are parallel fibers. Scale bar, 10 µm. The bar graph displays the distribution of GFP$^+$ cells in the different layers at P6 D4. Numbers in the bar represent animals used, and >800 neurons were counted per group. (*E*) P6 cerebella were electroporated with the indicated siRNAs and plasmids and collected at D4. GFP signals within the boxed regions are enlarged at the *bottom* (black). (Arrows) GFP$^+$ cells in the EGL. Scale bar, 20 µm. The bar graph shows the distribution of GFP$^+$ cells at P6 D4. Numbers in the bar represent animals used, and >600 neurons were counted per group.

examined the molecular signatures of the ectopic cells that remained in the EGL. At D4 after cerebellar electroporation, we observed more NeuN$^-$Tuj1$^-$ cells (Fig. 5A, B; Supplemental Fig. S6A) and more Ki67$^+$Tuj1$^-$ cells (Fig. 5C,D; Supplemental Fig. S6B) in *Kiaa0753* KD cerebella compared with si-control cerebella, suggesting that the cells remaining in the EGL upon *Kiaa0753* KD are still GNPs. Notably, the accumulation of Ki67$^+$Tuj1$^-$ and NeuN$^-$Tuj1$^-$ cells was effectively rescued by introducing human *KIAA0753* (pCIG2-h*KIAA0753*) (Fig. 5A–D; Supplemental Fig. S6A,B), confirming the specific effect of *Kiaa0753* KD.

We also tested whether Kiaa0753 regulates the differentiation of GNPs, as seen for Cep120 at D2 after cerebellar

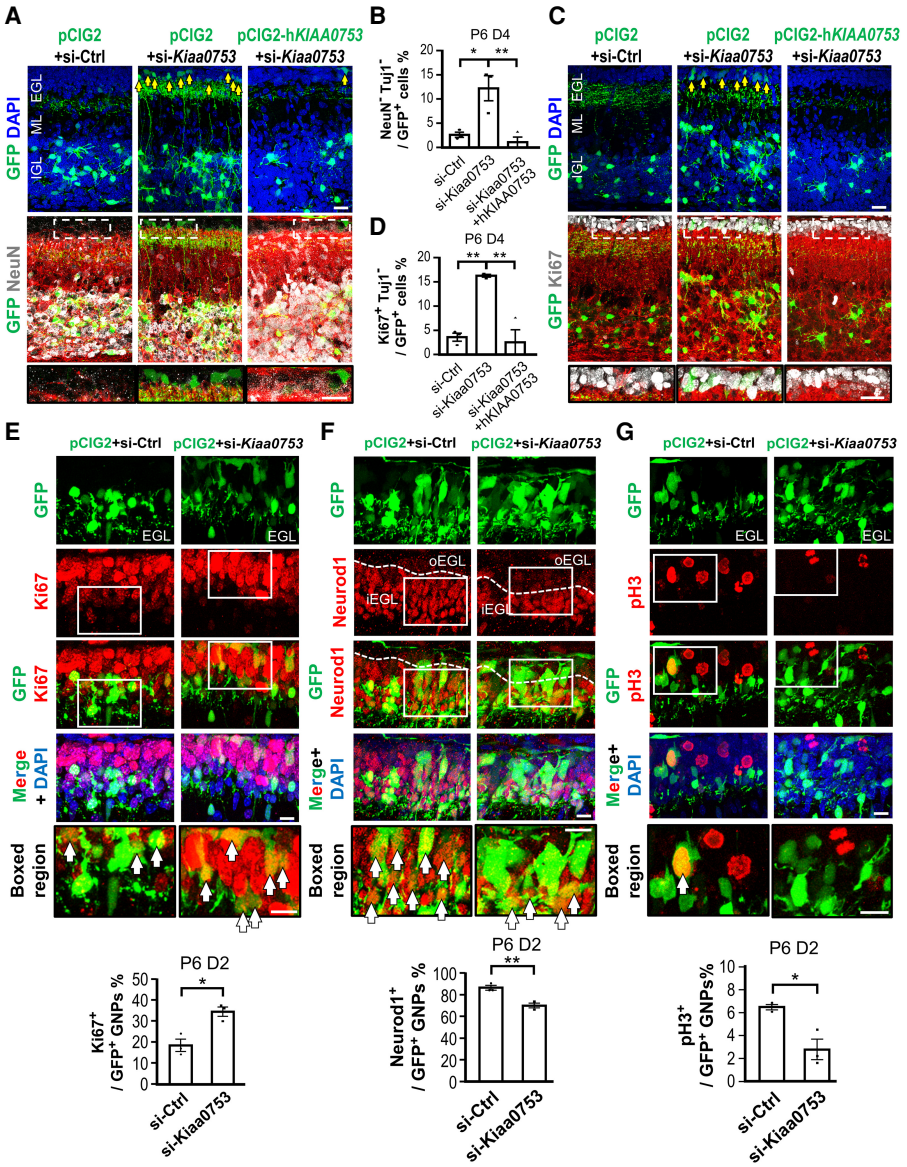

Figure 5. *Kiaa0753* KD phenocopies *Cep120* KD during cerebellar development. (*A–D*) P6 cerebella were electroporated with the indicated siRNAs and plasmids, collected at D4, and immunostained for NeuN or Ki67 (white in *A* or *C*), Tuj1 (red), and DAPI (blue). Boxed regions in the EGL are enlarged at the *bottom*. (Arrows) NeuN$^-$Tuj1$^-$ cells in *A* and Ki67$^+$ Tuj1$^-$ cells in *C*. Scale bar, 20 µm. The bar graphs represent the percentage of NeuN$^-$Tuj1$^-$ (*B*) or Ki67$^+$ Tuj1$^-$ (*D*) cells among the GFP$^+$ cells at D4. Three animals and >300 neurons were counted per group. (*E–G*) P6 cerebella were electroporated with the indicated siRNAs and plasmids and collected at D2. Cerebellar sections were immunostained for Ki67, Neurod1, or pH3 (red in *E–G*) and DAPI (blue). (Arrows) Ki67$^+$(*E*), Neurod1$^+$(*F*), and pH3$^+$ (*G*) cells among the GFP$^+$ cells. The dashed lines in *F* mark the boundary between the oEGL and iEGL. The boxed regions are enlarged at the *bottom* of each panel. Scale bar, 10 µm. The bar graphs show the percentage of Ki67$^+$ (*E*), Neurod1$^+$ (*F*), or pH3$^+$ (*G*) among the GFP$^+$ cells at D2. Three animals and >300 neurons were included per group.

electroporation in vivo. We found that depletion of Kiaa0753 in GNPs increased Ki67$^+$ cells (Fig. 5E) and reduced Neurod1$^+$ cells (Fig. 5F) compared with controls at D2, suggesting that *Kiaa0753* KD leads to increased retention of undifferentiated GNPs in the oEGL at D2 in vivo. The mitotic index, shown by the percentage of pH3$^+$ cells in the EGL, was also significantly reduced in *Kiaa0753* KD GNPs compared with control GNPs at D2 (Fig. 5G), indicating that *Kiaa0753* KD phenocopies *Cep120* KD in the developing cerebellum.

Moreover, we examined the expression of downstream Shh target genes in GNPs through RT-qPCR analysis and found that the ablation of the primary cilium by either *Kif3a* or *Ift88* KD (Chang et al. 2019) or knockdown of *Cep120*, *C2cd3*, *Talpid3*, or *Kiaa0753* (Supplemental Fig. S6C–F) suppressed the *Ptch1* and *Gli1* expression

upon smoothened agonist (SAG) stimulation (Supplemental Fig. S6G). However, *Cep120* or *Kiaa0753* KD maintained the expression of *Cyclin D1*, a signature of GNPs (Pogoriler et al. 2006), while its expression is reduced in *Talpid3* and *C2cd3* KD. This result suggests that although the primary cilium-mediated Shh signaling is reduced in GNPs with *Cep120* or *Kiaa0753* KD, these cells still kept their progenitor state in vitro.

Collectively, our results show that, similar to Cep120, Kiaa0753 participates in the neuronal differentiation and germinal zone exit of GNPs during cerebellar development.

CEP120 is required for the recruitment of KIAA0753 onto centrioles

Having shown that CEP120 forms protein complexes with KIAA0753 and both proteins are involved in regulating neuronal proliferation and differentiation in vivo, we hypothesized that Cep120 may be required for the recruitment of Kiaa0753 onto centrioles in proliferative cells. To test this possibility, we treated purified GNPs with SHH for 2 d to maintain cells in their proliferative state (Wallace 1999) prior to immunostaining. Our results showed that Kiaa0753 colocalized with γ-tubulin (a centrosomal protein marker) in proliferative GNPs in vitro, but that loss of Cep120 significantly decreased the centrosomal localization of Kiaa0753 signals (Fig. 6A,B). Notably, this effect was not due to a dramatic reduction of total Kiaa0753 proteins in GNPs upon *Cep120* KD (Fig. 6C). Furthermore, we discovered that Kiaa0753 proteins clustered at the base of primary cilia (marked by Arl13b positivity) in most GNPs (~60%) at D2 after electroporation in vivo (Supplemental Fig. S7A,B [A′ represents Arl13b$^+$ Kiaa0753 cluster]). Conversely, *Cep120* KD led not only to the loss of cilia from GNPs (Supplemental Fig. S1N–P), but also dispersion of these Kiaa0753 protein clusters (Supplemental Fig. S7A,B [A‴ represents Arl13b$^-$ Kiaa0753 disperse]). Collectively, these results suggest that Cep120 acts upstream for the recruitment of Kiaa0753 onto centrosomes in GNPs in vitro and in vivo.

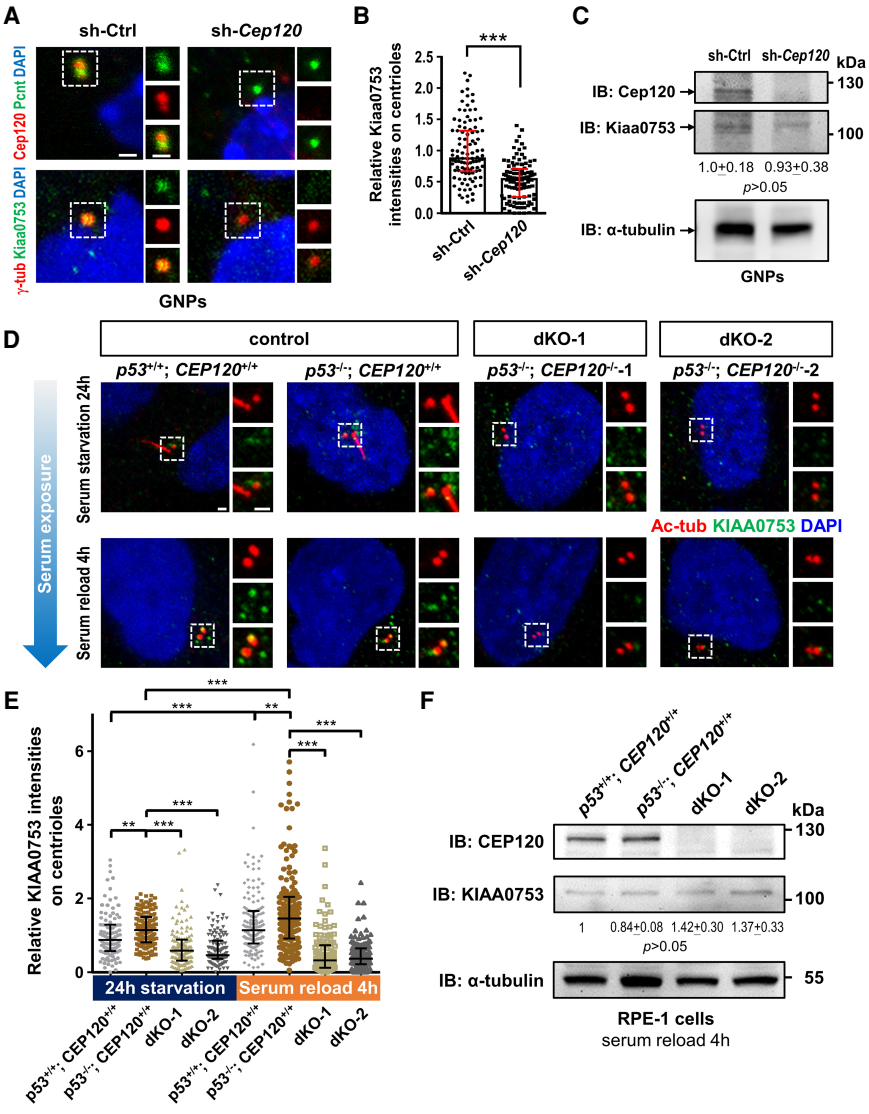

Figure 6. Loss of CEP120 hinders the recruitment of KIAA0753 onto centrioles. (*A*) P7 GNPs were infected with viruses carrying sh-Ctrl or sh-*Cep120* for 2 d and immunostained with Cep120 (red) and pericentrin (Pcnt, green) (*top* two panels) or γ-tubulin (γ-tub, red) and Kiaa0753 (green) (*bottom* two panels), and DAPI (blue). Scale bar, 1 µm. (*B*) Bar graph with scatter plots showing the relative Kiaa0753 intensities on centrioles of each GNP. More than 100 cells were counted per group. (*C*) Knockdown of Cep120 does not change the Kiaa0753 protein level. GNPs infected with viruses carrying the indicated shRNAs for 2 d and protein lysates were immunoblotted with the indicated antibodies. Numbers *below* the Kiaa0753 panel show the relative Kiaa0753 protein level by mean ± SEM. $n = 3$ trials. (*D*) RPE-1 cells of the indicated genotypes were serum-starved for 24 h (*top* four panels) and then serum was resupplied for 4 h (*bottom* four panels). Cells were immunostained with antibodies against acetylated tubulin (red), KIAA0753 (green), and DAPI (blue). The boxed regions with separated channels are enlarged at *right*. Scale bar, 1 µm. (*E*) The histogram displays the relative KIAA0753 intensities on centrioles *below* each condition. More than 100 cells were counted per group. (*F*) Knockout of CEP120 does not affect the KIAA0753 protein level. RPE-1 cell lysates were immunoblotted with the indicated antibodies. Cells were serum-starved for 24 h, and then serum was resupplied for 4 h. Numbers *below* the KIAA0753 panel show the relative KIAA0753 protein level as the mean ± SEM. $n = 3$ trials.

As KIAA0753 is known to regulate the G1–S phase transition during the cell cycle (Kodani et al. 2015), we examined whether CEP120 is required for the recruitment of KIAA0753 onto centrioles prior to this transition. Since GNPs are cultivated in serum-free SHH+ medium, they cannot be synchronized at G0/G1 phase. Therefore, we used two previously reported independent RPE1-based *CEP120/p53* double-knockout (dKO) cell lines: *CEP120*$^{-/-}$; *p53*$^{-/-}$-1 (here called dKO-1) and *CEP120*$^{-/-}$; *p53*$^{-/-}$-2 (here called dKO-2) (Tsai et al. 2019). After serum starvation for 24 h, which arrests most cells at G0/G1 phase, only a few KIAA0753 signals were detected on the centrioles of control cells (*p53*$^{+/+}$; *CEP120*$^{+/+}$ or *p53*$^{-/-}$; *CEP120*$^{+/+}$) and such signals were barely detected on dKO-1 or dKO-2 centrioles (Fig. 6D,E). Interestingly, after serum resupplementation for 4 h, which released the cells from G0/G1 stage, the KIAA0753 signal intensities were profoundly increased on centrioles of control cells, whereas these signals were still rarely detectable in dKO-1 and dKO-2 cells (Fig. 6D,E). Since the proportion of S-phase cells was not yet elevated at this time point (Supplemental Fig. S7C) and the KIAA0753 protein level was indistinguishable between control and *CEP120* KO cells (Fig. 6F), these results indicate that CEP120 is required for the recruitment of KIAA0753 onto centrioles prior to the G1-to-S phase transition.

The localization of KIAA0753 onto centrioles is required for the departure of GNPs from their germinal zone in vivo

Having observed that the centriolar localization of KIAA0753 is mediated by CEP120 (Fig. 6), we next sought to dissect the CEP120-interacting domain on KIAA0753. We transfected a series of FLAG-tagged KIAA0753 truncation constructs into HEK293T cells and found that the endogenous CEP120 could coimmunoprecipitate with full-length KIAA0753-FLAG and KIAA0753-FLAG (amino acids 1–300) (Supplemental Fig. S8A,B). To validate this result, we transfected these FLAG-tagged KIAA0753 truncation constructs into RPE-1 cells and performed cold treatment for 1 h to depolymerize intracellular microtubules, which facilitated visualizing their centrosomal localization. Once again, we observed that the FLAG signals from full-length KIAA0753-FLAG and KIAA0753-FLAG (amino acids 1–300) colocalized with CEP120 on centrioles (Supplemental Fig. S8C). These findings indicate that the N-terminal region of KIAA0753-FLAG is crucial for its interaction with CEP120.

To study whether Kiaa0753 functions downstream from Cep120 for the germinal zone exit of GNPs in the developing cerebellum, we exogenously expressed full-length KIAA0753 proteins in *Cep120* KD GNPs and looked for rescue of *Cep120* KD phenotypes. Reproducibly, *Cep120* KD resulted in the retention of more GFP$^+$ cells in the EGL (Supplemental Fig. S9A), which then possessed higher percentages of NeuN$^-$Tuj1$^-$ (Supplemental Fig. S9B,C) and Ki67$^+$Tuj1$^-$ (Supplemental Fig. S9D,E) progenitor cell signatures compared with controls. The reintroduction of full-length KIAA0753 (pCIG2-*KIAA0753*) reversed the accumulation of progenitor cells in the EGL; however, the introduction of N-terminal-truncated KIAA0753 (amino acids 301–967; termed pCIG2-KIAA0753ΔN), which was unable to form a complex with Cep120, did not rescue the defective germinal zone exit of GNPs in the developing cerebellum (Supplemental Fig. S9). Interestingly, Kiaa0753 signals could be detected surrounding Arl13b signals in most *Cep120* KD and Kiaa0753-overexpressing GNPs in vivo (Supplemental Fig. S9F), suggesting that excess Kiaa0753 proteins may take advantage of residual Cep120 or that an unknown compensate mechanism may be responsible for their localization to the base of primary cilia. Together, these results indicate that KIAA0753 functions downstream from Cep120 for the germinal zone exit of GNPs, and the interaction of these two proteins onto centrioles is substantial for this process.

JS-associated CEP120 mutants impair the recruitment of KIAA0753 onto centrioles and delay the departure of GNPs from the germinal zone

We next sought to map the KIAA0753-interacting domain on CEP120 by cotransfecting various myc-tagged *CEP120* truncated constructs with FLAG-tagged full-length *KIAA0753* into HEK293T cells. Our co-IP experiments narrowed down the KIAA0753-interacting domain to a specific C-terminal region on CEP120 (amino acids 442–894) (Fig. 7A).

A recent study showed that three *CEP120* missense mutations identified in JS (namely, A549V, L712F, and L726P) lead to severe developmental defects in the cerebellum (Roosing et al. 2016). Interestingly, these three disease-associated mutations are located within the KIAA0753–CEP120 interaction region (amino acids 442–894) (Fig. 7A). We thus investigated whether these mutations could affect the recruitment of KIAA0753 on centrioles. By taking advantage of established RPE1-based dKO-2 cells (*p53*$^{-/-}$; *CEP120*$^{-/-}$-2) (Tsai et al. 2019), we previously showed that inducibly expressed GFP-tagged CEP120 wild type (WT) or CEP120 mutants were associated with the production of extra long centrioles upon doxycycline treatment (Tsai et al. 2019). Interestingly, the endogenous KIAA0753 protein was detected along the elongated centrioles of cells expressing CEP120-WT-GFP, but such signals were markedly reduced in cells expressing the three JS-associated CEP120 mutants (Fig. 7B). Further co-IP experiments showed that the associations of these three CEP120 mutants with endogenous KIAA0753 were obviously reduced (Supplemental Fig. S10A). Together, our results indicate that the JS-associated mutations within this KIAA0753-interacting domain of CEP120 impair the recruitment of KIAA0753 onto centrioles.

Finally, to unravel the impacts of these three JS-associated *CEP120* mutations on cerebellar development, we reintroduced human CEP120 WT or each CEP120 mutant into *Cep120* KD GNPs in vivo. At D4 after electroporation, the expression of CEP120 WT promoted the germinal zone exit in *Cep120* KD GNPs, as evidenced by a decreased percentage of GFP$^+$ cells remaining in the

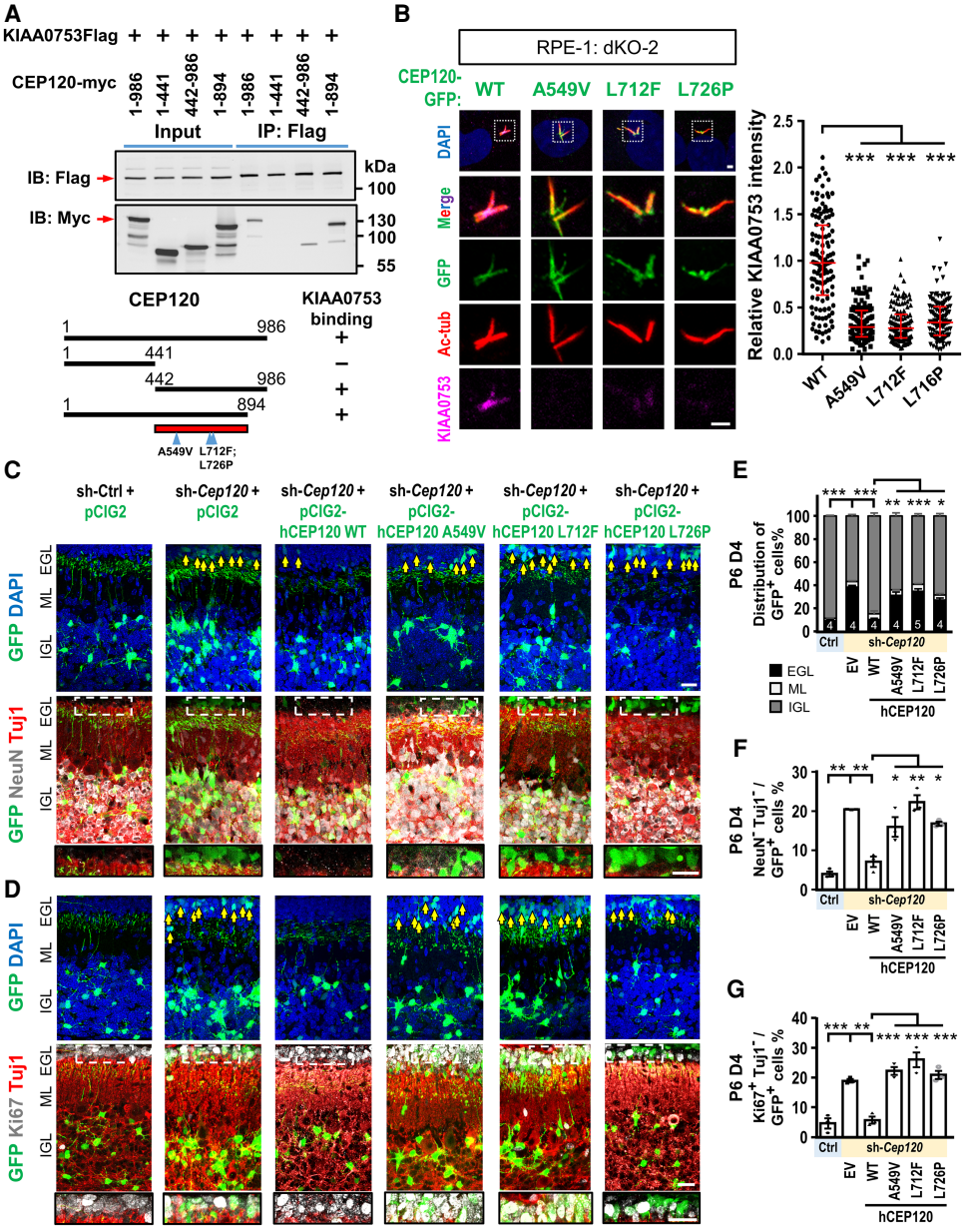

Figure 7. JS mutations in the *KIAA0753*-associated domain of *CEP120* cause defects in the germinal zone exit of GNPs. (*A*) HEK293T cells were cotransfected with FLAG-tagged KIAA0753 and various myc-tagged CEP120 constructs, followed by IP and IB with the indicated antibodies. Schematic diagram for the KIAA0753-interacting domains tested. The validated KIAA0753-associated domain of CEP120 is indicated in red. (Arrowheads) CEP120 mutants found in JS. (*B*) Disease-associated CEP120 mutants impair the recruitment of KIAA0753 to centrioles. $P53^{-/-}$; $CEP120^{-/-}$ (dKO)-2 cells with the indicated CEP120-GFP genotypes were serum-starved for 24 h and then serum was resupplied for 4 h. The cells were then immunostained for acetylated tubulin (red), KIAA0753 (magenta), and DAPI (blue). The boxed regions with separated channels are enlarged at the *bottom*. Scale bar, 2 µm. The histogram illustrates the relative intensities of KIAA0753 on CEP120-GFP$^+$ centrioles. More than 100 cells were counted per group. (*C*,*D*) P6 cerebella were electroporated with the indicated plasmids, collected at D4, and immunostained for NeuN or Ki67 (white in *C* or *D*), Tuj1 (red), and DAPI (blue). The boxed regions are enlarged at the *bottom*. (Arrows) NeuN$^-$ Tuj1$^-$ cells in *C* and Ki67$^+$ Tuj1$^-$ cells in *D*. Scale bar, 20 µm. (*E*–*G*) The bar graph displays the distribution of GFP$^+$ cells (*E*) and the percentage of NeuN$^-$Tuj1$^-$ cells (*F*) or Ki67$^+$Tuj1$^-$ cells (*G*) among all GFP$^+$ cells at D4. (EV) Empty vector. The numbers in the bar represent animals used, and >500 neurons were counted per group.

EGL (Fig. 7C–E), and enabled them to differentiate from the progenitor state (Fig. 7C–G; Supplemental Fig. S10B, C). Strikingly, the expression of the CEP120 mutants (A549V, L712F, or L726P) in *Cep120* KD GNPs neither decrease the accumulation of GNPs in the EGL nor promote the differentiation of Ki67$^+$Tuj1$^-$ or NeuN$^-$Tuj1$^-$ progenitor cells (Fig. 7C–G; Supplemental Fig. S10B,C). In conclusion, we found that these JS-associated

mutations within the KIAA0753-interacting region of CEP120 impair the recruitment of KIAA0753 onto centrioles in vitro and impede the departure of GNPs from their germinal zone in vivo.

Discussion

A new perspective for the pathogenesis of Joubert syndrome

JS is a genetically heterogeneous autosomal recessive ciliopathy that mainly impacts the development of the cerebellum and brain stem, which is reflected by a classical "molar tooth sign" (MTS) in neuroimaging (Romani et al. 2013). Deletion or mutations of the genes encoding ciliary proteins lead to cerebellar hypoplasia. Evidence suggests that this reflects in part a severe compromise in the primary cilia-mediated cellular response to SHH signaling (Chizhikov et al. 2007; Spassky et al. 2008; Aguilar et al. 2012). In line with this, the expression levels of Cyclin D1, Cyclin D2, and Cyclin E in GNPs are reportedly reduced upon ciliary loss (Kenney and Rowitch 2000), leading to a rapid disappearance of neural progenitors (Spassky et al. 2008).

In this study, we confirmed that depletion of the ciliopathy-associated genes *Cep120*, *Talpid3*, *C2cd3*, and *Kiaa0753* impairs the ciliogenesis of GNPs in vivo (Supplemental Figs. S1, S5). Among these genes, we surprisingly found that *Cep120* or *Kiaa0753* KD not only reduced the primary cilium-mediated Shh signaling in GNPs, but also maintained the expression of *Cyclin D1*, suggesting that *Cep120* or *Kiaa0753* KD may prolong the progenitor state. In line with this, we observed the accumulation of $Ki67^{+}Tuj1^{-}$ neural progenitor cells in the EGL in *Cep120* or *Kiaa0753* KD groups at D4, when most of the cells in the control group had already reached the IGL and begun expressing the mature neuronal marker, $NeuN^{+}Tuj1^{+}$ (Figs. 1, 5). Since expansion of the $Ki67^{+}$ population may represent either an increase of proliferative GNPs (Matsuo et al. 2013) or potentially a cell cycle arrest (van Oijen et al. 1998), we tested these possibilities. Our results showed that *Cep120* KD decreased S-phase-dependent EdU incorporation and reduced the mitotic events in GNPs in vivo and in vitro (Fig. 3; Supplemental Fig. S4), which supports a cell cycle arrest model. As mutations in *CEP120* and *KIAA0753* have been implicated in JS (Roosing et al. 2016; Stephen et al. 2017), our observations extend the complexity of "JS-associated ciliopathy" to include reduction of the primary cilia-mediated proliferative capability of GNPs and blockage of cell cycle progression, leading to impaired cerebellar neurogenesis in JS (Supplemental Fig. S11).

Historically, neuropathological examinations of JS patients revealed the accumulation of ectopic cells (termed heterotopia) in the cerebellar parenchyma, deep cerebellar nuclei, and subcortical regions (Friede and Boltshauser 1978; Yachnis and Rorke 1999; Juric-Sekhar et al. 2012). Among these, unorganized streaks of GNPs found in the EGL and decreased differentiation of the cerebellar cortex drew our attention, because they indicate that JS is not solely related to reduced neurogenesis; however, a more intricate etiology that would account for neuronal heterotopia and differentiation has not yet been elucidated. Although no report describes a careful neuropathological examination of cerebella obtained from JS patients carrying *CEP120* or *KIAA0753* mutations, our current report on the abnormal cerebellar features by depleting *Cep120* or *Kiaa0753* or introducing different *CEP120* mutants through in vivo cerebellar electroporation should provide valuable new insights into the pathogenesis of human JS.

The roles of Cep120 in the development of the CNS

Cep120 is highly expressed in embryonic mouse cerebral cortexes (Xie et al. 2007) and in the developing human cerebellum, especially in the EGL and ML at later stages (19PCW) when GNPs are actively proliferating (Powell et al. 2020). Thus, CEP120 appears to play key roles during the development of the CNS, particularly in radial glial (RG) cells of cerebral cortexes and in GNPs of developing cerebella. Although Cep120 functions as a centrosomal protein, we did not observe any change in leading process formation among migrating neurons or find defects in the neurite formation upon *Cep120* KD during cerebellar neurogenesis (Supplemental Fig. S12). Instead, we discovered that Cep120 participates in the timely differentiation in GNPs.

Interestingly, *Cep120* KD was reported to impair interkinetic nuclear migration (INM; a specialized behavior of RG cells during cell cycle progression), leading to decreases in the BrdU-labeling index and mitotic index of the developing cortex (Xie et al. 2007). Similarly, we found that *Cep120* KD decreased the EdU-labeling index at D1 and the mitotic index at D2 in GNPs of developing cerebellum (Fig. 3). However, unlike the behavior of RG cells in the developing cerebral cortex, we found that *Cep120* KD reduced the cell cycle exit of GNPs during cerebellar development (Fig. 2). This suggests that Cep120 plays divergent roles during neurogenesis, likely due to tissue-specific differences in the Cep120-interacting proteins. For example, Cep120 recruits TACC3 to the centrosome in RG cells, in which depletion of either protein was shown to disrupt INM and its coupled cell cycle progression, leading to a direct depletion of RG cells by cell cycle exit (Xie et al. 2007). In contrast, GNPs do not undergo INM, and TACC3 is not expressed in the cerebellum (Uhlén et al. 2015). As the differentiation of granule neurons depends on a proper cell cycle progression, which is required for the timely cell cycle exit (Espinosa and Luo 2008), here we identify a new Cep120-interacting protein, Kiaa0753 (Fig. 4), whose major roles are in cell cycle progression (Kodani et al. 2015) and GNP differentiation (Fig. 5). Thus, we conclude that Cep120 plays distinct roles in cell cycle exit in the developing cerebellum versus the cerebral cortex.

The role of KIAA0753 in cell cycle progression and the pathogenesis of JS

KIAA0753, which is also known as OFIP (OFD1- and FOPNL-interacting protein) or MNR (Moonraker), is a component of pericentriolar satellites that is capable of

forming complexes with other known satellite proteins, such as PCM1, OFD1, and FOR20 (Kodani et al. 2015; Chevrier et al. 2016). Notably, KIAA0753 has also been detected around pericentriolar regions at G1 phase; its fluorescence intensity was increased at S phase but gradually lost at metaphase (Kodani et al. 2015). Thus, KIAA0753 may participate in progressing the cell cycle from G1 to S phase. Interestingly, KIAA0753 was reported to promote centriole duplication by delivering WDR62 to centrosomes, which further induces the centrosomal localization of CEP63 with its binding partner, CDK2, for the G1–S phase transition (Kodani et al. 2015). Here, we show that KIAA0753 is detected at pericentriolar satellites and centrosomes in both RPE-1 cells (Fig. 6D) and GNPs (Fig. 6A). We further reveal that CEP120 interacts with the N-terminal (amino acids 1–300) centrosomal targeting domain of KIAA0753 (Supplemental Fig. S8) and functions upstream of KIAA0753 (Fig. 6). Importantly, depletion of Cep120 blocked the cell cycle transition and delayed the germinal zone exit of GNPs (Fig. 1). Collectively, we propose that the Cep120-mediated recruitment of Kiaa0753 to the centriole of GNPs is required for their differentiation and timely departure from the EGL in the developing cerebellum (Supplemental Fig. S11).

CEP120 and *KIAA0753* mutations have been independently identified in human patients with skeletal ciliopathies (Shaheen et al. 2015; Hammarsjo et al. 2017), JS (Roosing et al. 2016; Stephen et al. 2017), and oral–facial–digital syndrome (OFDS) type VI, a specific subgroup of OFDS in which the cerebellum is affected (Chevrier et al. 2016). Interestingly, we found that three JS-associated CEP120 missense mutants (p.A549V, p.L712F, and p.L726P) (Roosing et al. 2016) are located within the KIAA0753-interacting region (Fig. 7A), and lead to defective recruitment of KIAA0753 onto centrioles (Fig. 7B) and delayed departure of GNPs from their germinal zone (Fig. 7C). This suggests that the CEP120–KIAA0753 axis plays pivotal roles in the pathogenesis of JS.

In summary, we reveal here that the departure of GNPs from their germinal zone is mediated by the CEP120–KIAA0753 protein complex on centrioles, which facilitates proper cell cycle progression and neuronal differentiation in the developing cerebellum. Our findings provide a molecular basis for understanding the multifaceted neuropathology observed in ciliopathies of the developing cerebellum.

Materials and methods

Animal husbandry

CD-1 (RjOrl:SWISS) was purchased from the National Laboratory Animal Center in Taiwan. All animal procedures were performed according to the guidelines approved by the Institutional Animal Care and Use Committee (IACUC) of Academia Sinica.

Cell lines

HEK293T (ATCC CRL-3216) and hTERT-immortalized RPE-1 (ATCC CRL-4000) cells were cultured in Dulbecco's modified Eagle's medium (DMEM) or DMEM/F12 as described (Tsai et al. 2019). The RPE1-based doxycycline-inducible cell lines expressing CEP120-GFP (WT or A549V, L712F, or L726P mutants) and CEP120 knockout cells were generated and cultured as previously described (Tsai et al. 2019).

GNP primary cultures

P6 or P7 cerebellar GNPs were purified from a Percoll gradient as previously described (Zhao et al. 2008). GNPs were cultured in neurobasal-based medium containing 1% SHH-N terminus recombinant protein (R&D 461-SH-025) or 150 nM smoothened agonist (SAG; Enzo Life Sciences) as previously described (Zhao et al. 2008).

Cerebellar electroporation in vivo

In vivo cerebellar electroporation was performed as previously described (Chang et al. 2019). The experimental procedures were approved by the Institutional Animal Care and Use Committee (IACUC) of Academia Sinica. For details, see the Supplemental Material.

Plasmids and siRNA

For in vivo cerebellar electroporation, the rescue constructs pCIG2-*CEP120* and pCIG2-*KIAA0753* were used to express human CEP120 or KIAA0753 in sh-*Cep120* or sh-*Kiaa0753* knockdown cells, respectively, while pCIG2 vector was used as a control. The mutations of human *CEP120* (A549V, L712F, and L726P) with or without a FLAG tag were also subcloned into the pCIG2 vector for immunoprecipitation or in vivo electroporation, respectively. The pEGFP-N3-*CSPP1* and *CSPPL* plasmids were generous gifts from Dr. Sebastian Patzke (Patzke et al. 2006). The GFP-tagged *TALPID3* and *C2CD3* constructs (Tsai et al. 2019) and various myc-tagged *CEP120* truncated constructs (Lin et al. 2013) were as described previously. The cDNAs encoding various domains of *KIAA0753* were subcloned into the pCIG2 vector for this study. Short hairpin RNAs were derived from the RNAi Core in Taiwan, and then subcloned into a GFP-expressing vector (TRC011). Details for the shRNA and siRNA targeting sequences are listed in Supplemental Tables S1 and S2.

Generation of RPE1-based doxycycline-inducible cell lines

We previously generated RPE1-based cells inducibly expressing CEP120-GFP (WT and L712F and L726P mutants) (Tsai et al. 2019). A similar approach was used to generate RPE1-based cells inducibly expressing the CEP120-GFP (A549V) mutant. For details, see the Supplemental Material.

Virus production and Lipofectamine transfection

Viruses were generated as previously described (Chang et al. 2019). RPE-1 and HEK293T cells were transfected with Lipofectamine 2000 (Invitrogen) in accordance with the manufacturer's protocol.

Immunofluorescence and imaging

The cerebella were collected at the indicated timing. Sagittal sections of cerebella (100 µm) were produced using a vibratome (Leica VT1000S). Primary antibodies (Supplemental Table S3) and secondary antibodies (1:500; Alexa fluor; Thermo Fisher Scientific) were applied for 2 h at room temperature and counterstained with DAPI (Invitrogen) for 1 h. The slices were

mounted with VectaShield mounting solution (Vector Laboratories). To identify KIAA0753 signals on centrioles, GNPs or RPE-1 cells on coverslips were cold-treated for 1 h at 4°C, fixed in cold methanol at −20°C, and immunostained with primary antibodies and secondary antibodies for 2 h each at room temperature.

Microscopy

Cerebellar slices or cells were imaged under a laser scanning confocal microscope (LSM-700 stage, Zeiss) at a resolution of 1024 × 1024 with a 100× objective (N.A 1.4 oil, Zeiss). The excitation wavelengths were 405 nm for DAPI, 488 nm for EGFP, 555 nm for red fluorescence, and 639 nm for infrared fluorescence imaging.

Organotypic slice culture

P6 cerebella were electroporated with sh-Ctrl or sh-*Cep120* #1 and collected after 1 d. Cerebellar slices were made and cultured as previously described (Tsai et al. 2007). The slices were imaged under a Cell Observer system (Zeiss) with 5% CO_2 and steady temperature control at 37°C.

Image analysis and fluorescent intensity quantification

We used the ImageJ software (NIH) for detecting the length of Arl13b-labeled cilia, the length of neurites, and the fluorescent intensities of KIAA0753 on centrioles in GFP^+ cells. We used γ-tubulin and acetylated-tubulin as centrosomal markers for GNPs and RPE-1 cells, respectively, and measured the signal intensities of KIAA0753 within the centrosomal regions.

Immunoblotting

GNPs, RPE-1 cells, or HEK293T cells were lysed in RIPA buffer and mixed with a protease inhibitor cocktail (Sigma Aldrich) as described previously (Tsai et al. 2019). Proteins were analyzed by a BCA assay (Pierce) and then subjected to immunoblotting.

Immunoprecipitation

HEK293T cells were transfected with the indicated plasmids for 1 d and lysed in RIPA buffer with protease inhibitors. GNPs were isolated from P7 cerebella and lysed in T-PER tissue protein extraction reagent (Thermo Scientific). Samples were subjected to centrifugation at 15,000 rpm for 15 min, and the supernatants were immunoprecipitated and immunoblotted with the indicated antibodies as described (Tsai et al. 2019).

Cell cycle exit assay and cell cycle progression assay

EdU (Thermo Fisher Scientific C10338) was injected into mice at 50 mg/kg as described (Zeng et al. 2010). For the cell cycle exit assay, cerebella were electroporated with the indicated constructs at P6 (D0), and EdU reagents were injected subcutaneously at D1 after electroporation. Cerebella were collected at D2 and subjected to Ki67 immunostaining. The index for cell cycle exit was calculated as the percentage of $Ki67^-$ neurons among the GFP^+EdU^+ cells, as previously described (Sanada and Tsai 2005). For the cell cycle progression assay in vivo, cerebella were treated as described above for D0 and D1. Cerebella were collected at 3 h (+3 h) after EdU administration, and pH3 immunostaining was performed. For the cell cycle progression assay in vitro, GNPs were isolated from P7 cerebella. SAG (150 nM; Enzo Life Sciences) and lentiviruses carrying the indicated sh-RNAs were added to the GNPs 1 d after plating. EdU was added for 4 h at 3 d after virus infection. The analysis of cell cycle phases in GNPs in vivo and in vitro was performed as previously described (Florio et al. 2012).

RT-qPCR

GNPs were isolated from P7 cerebella, and SAG along with lentiviruses carrying the indicated shRNAs were added from DIV1 to DIV3 during the whole culture process. The GNPs were lysed at DIV4, and RNAs were extracted by RNA isolation kits as described by the manufacturer's protocol (Zymo Research). cDNAs were generated by iScript reverse transcription supermix (Bio-Rad), and SYBR Green PCR master mix (Thermo Fisher Scientific) was applied for RT-qPCR as described by the vendor's protocol. Primers for RT-qPCR analysis are listed in Supplemental Table S4.

Quantification and statistical analysis

We used the GraphPad Prism software (version 5.0), Excel software (Microsoft), and PASW Statistics 18 (IBM) to test for statistical significance and visualize the experimental results. All data are shown as mean ± SEM unless otherwise specified in the figure legend. We tested the normality of all data with the Kolmogorov–Smirnov test. The Student's *t* test was used to compare two groups with normal distribution (Figs. 3B,C, 4D, 5E–G, 6C), while the Mann–Whitney *U*-test was used to compare two groups with nonparametric data (Fig. 6B). For multiple groups with normal distribution, one-way ANOVA (Figs. 1A–C, 2B,C, 3E,H–J, 4E, 5A–D, 6F) and two-way ANOVA (Fig. 7E–G) were used for one or two categorical variables, respectively, and the LSD test or Bonferroni test was used for post-hoc analysis. For multiple groups with nonparametric distribution, we used the Kruskal–Wallis test (Figs. 6E, 7B). We considered statistical significance once $P < 0.05$ (not significant [N.S.], $P < 0.05$ [*], $P < 0.01$ [**], and $P < 0.001$ [***]).

Competing interest statement

The authors declare no competing interests.

Acknowledgments

We thank the Sequencing Core Facility (Institute of Biomedical Science [IBMS], AS-CFII-108-115) and the Confocal Imaging Core Facilities (IBMS, Neuroscience Program of Academia Sinica, Agriculture Biotechnology Research Center, AS-CFII-108-116) of Academia Sinica. We especially thank Nien-Tzu Lee for mouse colony management, Show-Rong Ma for confocal imaging assistance, and Tzu-Wen Tai for assistance with the flow cytometry. We thank Dr. Sebastian Patzke for providing plasmids encoding *CSPP1* and *CSPPL*. This work was funded by grants from the Ministry of Science and Technology, Taiwan (MOST-108-2321-B001-026) and Academia Sinica, Taiwan (AS-IA-109-L04; AS-TP-108-L08).

Author contributions: T.K.T., and C.-H.C. conceived the study, C.-H.C., T.-Y.C., I.-L.L., R.-B.L., J.-J.T., and P.-Y.L. performed the methodology. C.-H.C. T.-Y.C., I.-L.L., R.-B.L., J.-J.T., and T.K.T. performed the formal analysis. and investigation. C.-H.C. and T.K.T. wrote the original draft of the manuscript. C.-H.C. T.-Y.C., I.-L.L., R.-B.L., J.-J.T., P.-Y.L., and T.K.T. reviewed and edited the manuscript. T.K.T. supervised the study, was the project administrator, and acquired funding.

References

Aguilar A, Meunier A, Strehl L, Martinovic J, Bonniere M, Attie-Bitach T, Encha-Razavi F, Spassky N. 2012. Analysis of human samples reveals impaired SHH-dependent cerebellar development in Joubert syndrome/Meckel syndrome. *Proc Natl Acad Sci* **109:** 16951–16956. doi:10.1073/pnas.1201408109

Braun DA, Hildebrandt F. 2017. Ciliopathies. *Cold Spring Harb Perspect Biol* **9:** a028191. doi:10.1101/cshperspect.a028191

Chang CH, Zanini M, Shirvani H, Cheng JS, Yu H, Feng CH, Mercier AL, Hung SY, Forget A, Wang CH, et al. 2019. Atoh1 controls primary cilia formation to allow for SHH-triggered granule neuron progenitor proliferation. *Dev Cell* **48:** 184–199.e5. doi:10.1016/j.devcel.2018.12.017

Chevrier V, Bruel AL, Van Dam TJ, Franco B, Lo Scalzo M, Lembo F, Audebert S, Baudelet E, Isnardon D, Bole A, et al. 2016. OFIP/KIAA0753 forms a complex with OFD1 and FOR20 at pericentriolar satellites and centrosomes and is mutated in one individual with oral-facial-digital syndrome. *Hum Mol Genet* **25:** 497–513. doi:10.1093/hmg/ddv488

Chizhikov VV, Davenport J, Zhang Q, Shih EK, Cabello OA, Fuchs JL, Yoder BK, Millen KJ. 2007. Cilia proteins control cerebellar morphogenesis by promoting expansion of the granule progenitor pool. *J Neurosci* **27:** 9780–9789. doi:10.1523/JNEUROSCI.5586-06.2007

Comartin D, Gupta GD, Fussner E, Coyaud E, Hasegan M, Archinti M, Cheung SW, Pinchev D, Lawo S, Raught B, et al. 2013. CEP120 and SPICE1 cooperate with CPAP in centriole elongation. *Curr Biol* **23:** 1360–1366. doi:10.1016/j.cub.2013.06.002

Dahmane N, Ruiz-i-Altaba A. 1999. Sonic hedgehog regulates the growth and patterning of the cerebellum. *Development* **126:** 3089–3100. doi:10.1242/dev.126.14.3089

Edmondson JC, Hatten ME. 1987. Glial-guided granule neuron migration in vitro: a high-resolution time-lapse video microscopic study. *J Neurosci* **7:** 1928–1934. doi:10.1523/JNEUROSCI.07-06-01928.1987

Espinosa JS, Luo L. 2008. Timing neurogenesis and differentiation: insights from quantitative clonal analyses of cerebellar granule cells. *J Neurosci* **28:** 2301–2312. doi:10.1523/JNEUROSCI.5157-07.2008

Florio M, Leto K, Muzio L, Tinterri A, Badaloni A, Croci L, Zordan P, Barili V, Albieri I, Guillemot F, et al. 2012. Neurogenin 2 regulates progenitor cell-cycle progression and Purkinje cell dendritogenesis in cerebellar development. *Development* **139:** 2308–2320. doi:10.1242/dev.075861

Fraser AM, Davey MG. 2019. TALPID3 in Joubert syndrome and related ciliopathy disorders. *Curr Opin Genet Dev* **56:** 41–48. doi:10.1016/j.gde.2019.06.010

Friede RL, Boltshauser E. 1978. Uncommon syndromes of cerebellar vermis aplasia. I: Joubert syndrome. *Dev Med Child Neurol* **20:** 758–763. doi:10.1111/j.1469-8749.1978.tb15307.x

Fujita S. 1967. Quantitative analysis of cell proliferation and differentiation in the cortex of the postnatal mouse cerebellum. *J Cell Biol* **32:** 277–287. doi:10.1083/jcb.32.2.277

Garcez PP, Diaz-Alonso J, Crespo-Enriquez I, Castro D, Bell D, Guillemot F. 2015. Cenpj/CPAP regulates progenitor divisions and neuronal migration in the cerebral cortex downstream of Ascl1. *Nat Commun* **6:** 6474. doi:10.1038/ncomms7474

Gupta GD, Coyaud E, Goncalves J, Mojarad BA, Liu Y, Wu Q, Gheiratmand L, Comartin D, Tkach JM, Cheung SW, et al. 2015. A dynamic protein interaction landscape of the human centrosome-cilium interface. *Cell* **163:** 1484–1499. doi:10.1016/j.cell.2015.10.065

Hammarsjo A, Wang Z, Vaz R, Taylan F, Sedghi M, Girisha KM, Chitayat D, Neethukrishna K, Shannon P, Godoy R, et al. 2017. Novel KIAA0753 mutations extend the phenotype of skeletal ciliopathies. *Sci Rep* **7:** 15585. doi:10.1038/s41598-017-15442-1

Hatten ME, Roussel MF. 2011. Development and cancer of the cerebellum. *Trends Neurosci* **34:** 134–142. doi:10.1016/j.tins.2011.01.002

Hendzel MJ, Wei Y, Mancini MA, Van Hooser A, Ranalli T, Brinkley BR, Bazett-Jones DP, Allis CD. 1997. Mitosis-specific phosphorylation of histone H3 initiates primarily within pericentromeric heterochromatin during G2 and spreads in an ordered fashion coincident with mitotic chromosome condensation. *Chromosoma* **106:** 348–360. doi:10.1007/s004120050256

Hoover AN, Wynkoop A, Zeng H, Jia J, Niswander LA, Liu A. 2008. C2cd3 is required for cilia formation and Hedgehog signaling in mouse. *Development* **135:** 4049–4058. doi:10.1242/dev.029835

Juric-Sekhar G, Adkins J, Doherty D, Hevner RF. 2012. Joubert syndrome: brain and spinal cord malformations in genotyped cases and implications for neurodevelopmental functions of primary cilia. *Acta Neuropathol* **123:** 695–709. doi:10.1007/s00401-012-0951-2

Kenney AM, Rowitch DH. 2000. Sonic hedgehog promotes G_1 cyclin expression and sustained cell cycle progression in mammalian neuronal precursors. *Mol Cell Biol* **20:** 9055–9067. doi:10.1128/MCB.20.23.9055-9067.2000

Kodani A, Yu TW, Johnson JR, Jayaraman D, Johnson TL, Al-Gazali L, Sztriha L, Partlow JN, Kim H, Krup AL, et al. 2015. Centriolar satellites assemble centrosomal microcephaly proteins to recruit CDK2 and promote centriole duplication. *Elife* **4:** e07519. doi:10.7554/eLife.07519

Lin YN, Wu CT, Lin YC, Hsu WB, Tang CJ, Chang CW, Tang TK. 2013. CEP120 interacts with CPAP and positively regulates centriole elongation. *J Cell Biol* **202:** 211–219. doi:10.1083/jcb.201212060

Lin YN, Lee YS, Li SK, Tang TK. 2020. Loss of CPAP in developing mouse brain and its functional implication for human primary microcephaly. *J Cell Sci* **133:** jcs243592. doi:10.1242/jcs.243592

Mahjoub MR, Xie Z, Stearns T. 2010. Cep120 is asymmetrically localized to the daughter centriole and is essential for centriole assembly. *J Cell Biol* **191:** 331–346. doi:10.1083/jcb.201003009

Matsuo S, Takahashi M, Inoue K, Tamura K, Irie K, Kodama Y, Nishikawa A, Yoshida M. 2013. Thickened area of external granular layer and Ki-67 positive focus are early events of medulloblastoma in Ptch1$^{+/-}$ mice. *Exp Toxicol Pathol* **65:** 863–873. doi:10.1016/j.etp.2012.12.005

Nakashima K, Umeshima H, Kengaku M. 2015. Cerebellar granule cells are predominantly generated by terminal symmetric divisions of granule cell precursors. *Dev Dyn* **244:** 748–758. doi:10.1002/dvdy.24276

Patzke S, Stokke T, Aasheim HC. 2006. CSPP and CSPP-L associate with centrosomes and microtubules and differently affect microtubule organization. *J Cell Physiol* **209:** 199–210. doi:10.1002/jcp.20725

Pogoriler J, Millen K, Utset M, Du W. 2006. Loss of cyclin D1 impairs cerebellar development and suppresses medulloblastoma formation. *Development* **133:** 3929–3937. doi:10.1242/dev.02556

Powell L, Barroso-Gil M, Clowry GJ, Devlin LA, Molinari E, Ramsbottom SA, Miles CG, Sayer JA. 2020. Expression patterns of ciliopathy genes ARL3 and CEP120 reveal roles in multisystem development. *BMC Dev Biol* **20:** 26. doi:10.1186/s12861-020-00231-3

Romani M, Micalizzi A, Valente EM. 2013. Joubert syndrome: congenital cerebellar ataxia with the molar tooth. *Lancet Neurol* **12:** 894–905. doi:10.1016/S1474-4422(13)70136-4

Roosing S, Romani M, Isrie M, Rosti RO, Micalizzi A, Musaev D, Mazza T, Al-Gazali L, Altunoglu U, Boltshauser E, et al. 2016. Mutations in *CEP120* cause Joubert syndrome as well as complex ciliopathy phenotypes. *J Med Genet* **53:** 608–615. doi:10.1136/jmedgenet-2016-103832

Sanada K, Tsai LH. 2005. G protein βγ subunits and AGS3 control spindle orientation and asymmetric cell fate of cerebral cortical progenitors. *Cell* **122:** 119–131. doi:10.1016/j.cell.2005.05.009

Shaheen R, Schmidts M, Faqeih E, Hashem A, Lausch E, Holder I, Superti-Furga A, Mitchison HM, Almoisheer A, Alamro R, et al. 2015. A founder CEP120 mutation in Jeune asphyxiating thoracic dystrophy expands the role of centriolar proteins in skeletal ciliopathies. *Hum Mol Genet* **24:** 1410–1419. doi:10.1093/hmg/ddu555

Spassky N, Han YG, Aguilar A, Strehl L, Besse L, Laclef C, Ros MR, Garcia-Verdugo JM, Alvarez-Buylla A. 2008. Primary cilia are required for cerebellar development and Shh-dependent expansion of progenitor pool. *Dev Biol* **317:** 246–259. doi:10.1016/j.ydbio.2008.02.026

Stephen J, Vilboux T, Mian L, Kuptanon C, Sinclair CM, Yildirimli D, Maynard DM, Bryant J, Fischer R, Vemulapalli M, et al. 2017. Mutations in KIAA0753 cause Joubert syndrome associated with growth hormone deficiency. *Hum Genet* **136:** 399–408. doi:10.1007/s00439-017-1765-z

Tsai JW, Bremner KH, Vallee RB. 2007. Dual subcellular roles for LIS1 and dynein in radial neuronal migration in live brain tissue. *Nat Neurosci* **10:** 970–979. doi:10.1038/nn1934

Tsai JJ, Hsu WB, Liu JH, Chang CW, Tang TK. 2019. CEP120 interacts with C2CD3 and Talpid3 and is required for centriole appendage assembly and ciliogenesis. *Sci Rep* **9:** 6037. doi:10.1038/s41598-019-42577-0

Uhlén M, Fagerberg L, Hallström BM, Lindskog C, Oksvold P, Mardinoglu A, Sivertsson Å, Kampf C, Sjöstedt E, Asplund A, et al. 2015. Proteomics. tissue-based map of the human proteome. *Science* **347:** 1260419. doi:10.1126/science.1260419

van Oijen MG, Medema RH, Slootweg PJ, Rijksen G. 1998. Positivity of the proliferation marker Ki-67 in noncycling cells. *Am J Clin Pathol* **110:** 24–31. doi:10.1093/ajcp/110.1.24

Wallace VA. 1999. Purkinje-cell-derived Sonic hedgehog regulates granule neuron precursor cell proliferation in the developing mouse cerebellum. *Curr Biol* **9:** 445–448. doi:10.1016/S0960-9822(99)80195-X

Wang L, Failler M, Fu W, Dynlacht BD. 2018. A distal centriolar protein network controls organelle maturation and asymmetry. *Nat Commun* **9:** 3938. doi:10.1038/s41467-018-06286-y

Wechsler-Reya RJ, Scott MP. 1999. Control of neuronal precursor proliferation in the cerebellum by Sonic Hedgehog. *Neuron* **22:** 103–114. doi:10.1016/S0896-6273(00)80682-0

Woods CG, Bond J, Enard W. 2005. Autosomal recessive primary microcephaly (MCPH): a review of clinical, molecular, and evolutionary findings. *Am J Hum Genet* **76:** 717–728. doi:10.1086/429930

Wu C, Yang M, Li J, Wang C, Cao T, Tao K, Wang B. 2014. Talpid3-binding centrosomal protein Cep120 is required for centriole duplication and proliferation of cerebellar granule neuron progenitors. *PLoS One* **9:** e107943. doi:10.1371/journal.pone.0107943

Xie Z, Moy LY, Sanada K, Zhou Y, Buchman JJ, Tsai LH. 2007. Cep120 and TACCs control interkinetic nuclear migration and the neural progenitor pool. *Neuron* **56:** 79–93. doi:10.1016/j.neuron.2007.08.026

Yachnis AT, Rorke LB. 1999. Neuropathology of Joubert syndrome. *J Child Neurol* **14:** 655–659; discussion 669-672. doi:10.1177/088307389901401006

Zeng C, Pan F, Jones LA, Lim MM, Griffin EA, Sheline YI, Mintun MA, Holtzman DM, Mach RH. 2010. Evaluation of 5-ethynyl-2′-deoxyuridine staining as a sensitive and reliable method for studying cell proliferation in the adult nervous system. *Brain Res* **1319:** 21–32. doi:10.1016/j.brainres.2009.12.092

Zhao H, Ayrault O, Zindy F, Kim JH, Roussel MF. 2008. Post-transcriptional down-regulation of Atoh1/Math1 by bone morphogenic proteins suppresses medulloblastoma development. *Genes Dev* **22:** 722–727. doi:10.1101/gad.1636408